AIAA SciTech Forum
8–12 January 2018, Kissimmee, Florida
2018 AIAA Information Systems-AIAA Infotech @ Aerospace
10.2514/6.2018-0250

Modeling and Control of Quadrotor Formations Carrying a Slung Load

Segun Olumide Ariyibi[1] and Ozan Tekinalp[2]
Middle East Technical University, Ankara, 06800, Turkey

Equations of motion of a two quadrotor carrying a slung load is developed using a multibody dynamics approach. Its extension to three quadrotors carrying a slung load is also presented. The rope attaching the quadrotor to the load is assumed to be rigid. A Lyapunov function based guidance algorithm is designed to fly the quadrotors in formation. Linear quadratic tracking controllers are used for the quadrotors. The simulation results indicate that the controller performs well under the disturbance of the slinging load.

Nomenclature

ω_i	=	quadrotor i angular velocity, written in quadrotor i fixed frame. $i=1,2$
ω_L	=	angular velocity of the load with respect to the inertial frame.
ω_{c_i}	=	angular velocity of the cable i with respect to the inertial frame. $i=1,2$
T_i	=	torque acting on the quadrotor i . $i=1,2$
T_{S_i}	=	friction and damping torques at the joints. $i=1,2,3,4$
C_N^i	=	the direction cosine matrix from the inertial frame to quadrotor i frame.
C_N^L	=	the direction cosine matrix from the inertial frame to the load frame.
$C_N^{c_i}$	=	the direction cosine matrix from the inertial frame to cable i frame.
F_{S_i}	=	the reaction force at the spherical joints connecting the quadrotors, cables and Load. $i=1,2,3,4$
$\omega_1^{\times}$	=	matrix to carry out cross product, $\omega_1 \times r_1 = \omega_1^{\times} r_1$
$\omega_1^{\times\times}$	=	matrix to carry out cross product: $\omega_1 \times (\omega_1 \times r_1) = \omega_1^{\times\times} r_1$
f_i	=	Force generated by the ith rotor.
t_i	=	Torque generated by the ith rotor.
d	=	Level Arm.
U_i	=	Quadrotor control inputs.

I. Introduction

UAVs find thier use in search and rescue missions, disaster relief operations, environmental monitoring, and surveilance. Such diverse missions place severe demands on the design of control systems that can adapt to different scenarios and possible changes of vehicle dynamics. Carrying a slung load is one such application changing the dynamics of the vehicle and making the control difficult[1]. A quadrotor is a rotary-wing UAV with hovering and vertical take-off and landing (VTOL) capabilities. Its dynamics is much simpler than that of a

[1] Ph.D. Student, Department of Aerospace Engineering.
[2] Professor, Department of Aerospace Engineering, and AIAA Senior Member.

helicopter enjoying the interest of researchers over many years. Many linear controllers,[2] adaptive controllers,[3] backstapping control etc.[4] have been proposed to control a quadrotor.

The work reported here is on the modeling and control of two and three UAV's flying in formation and carrying a slung load (also known as sling load or suspended load) cooperatively. Guidance and control of aircraft flying in formation has been addressed previously.[5,6]

Flying a quadrotor with a slung load has not been extensively investigated in the literature.[1] The slung load dynamics significantly alters the flying characteristics of the quadrotor, presenting a challenge in controlling the UAV. The additional degrees of freedom of the load dynamics also signaficantly complicate the equations of motion of the quadrotor-slung load system. In this paper, the approach presented by Stoneking[7] for multi-body spacecrafts is employed to model our two quadrotor slung load system. The building block equations are derived by applying Newton's and Euler's equations of motion to an "element" consisting of five bodies and four joints. In this case, the five bodies are the two quadrotors, the two cables connecting the quadrotor to the load and the load; the four joints are spherical joints through which the cables connect the quadrotors to the load. Straightforward linear algebra operations are employed to eliminate extraneous constraint equations, resulting in a minimum-dimension system of equations to solve. This method thus combines a straightforward, easily-extendable, easily-mechanized formulation with an efficient computer implementation. The approach is also extended to three quadrotor formation carrying a slung load case.

In the following, the two quadrotor with a slung load system modeling is given first, followed by a discussion on its extension to a three quadrotor formation case. The presentation of quadrotor equations of motion and the linear quadratic tracking control methodology employed is given next. Then the Lyapuınov function based formation guidance control methodology is presented. Simulation results are given and discussed. Finally conclusions are given.

II. Equation of motion for the quadrotor-suspended load system

A. Two Quadrotors With a Suspended Load

We assume that the cables connecting the quadrotors to the load are stiff, and with relatively negligible masses. They are attached to the quadrotors and load with a spherical joint. The joint torques, may be assumed zero. Using the approach of Stoneking,[7] the equations of motion are derived. The rotational euqations for the two quadrotors in their quadrotor fixed frame:

$$\begin{aligned} J_1\dot{\omega}_1 &= T_1 + T_{S_1} - \omega_1^{\times} J_1 \omega_1 + r_1^{\times} C_N^1 F_{S_1} \\ J_2\dot{\omega}_2 &= T_2 - C_{c_2}^2 T_{S_4} - r_2^{\times} C_N^2 F_{S_4} - \omega_2^{\times} J_2 \omega_2 \end{aligned} \tag{1}$$

Similarly, the rotational equations of motion of the load in its own frame as well as the cables in their reference frames are:

$$\begin{aligned} J_{c_1}\dot{\omega}_{c_1} &= T_{c_1} - C_1^{c_1} T_{S_1} - r_{c_{11}}^{\times} C_N^{c_1} F_{S_1} + T_{s_2} + r_{c_{12}}^{\times} C_N^{c_1} F_{S_2} - \omega_{c_1}^{\times} J_{c_1} \omega_{c_1} \\ J_L\dot{\omega}_L &= T_L - C_{c_1}^L T_{s_2} - r_{L_1}^{\times} C_N^L F_{S_2} + T_{s_3} + r_{L_2}^{\times} C_N^L F_{S_3} - \omega_L^{\times} J_L \omega_L \\ J_{c_2}\dot{\omega}_{c_2} &= T_{c_2} - C_L^{c_2} T_{S_3} - r_{c_{21}}^{\times} C_N^{c_2} F_{S_3} + T_{s_4} + r_{c_{22}}^{\times} C_N^{c_2} F_{S_4} - \omega_{c_2}^{\times} J_{c_2} \omega_{c_2} \end{aligned} \tag{2}$$

The translational equations are written in the inertial frame:

$$\begin{aligned} m_1\dot{v}_1 &= F_1 + F_{S_1} \\ m_{c_1}\dot{v}_{c_1} &= F_{c_1} + F_{s_2} - F_{S_1} \\ m_L\dot{v}_L &= F_L + F_{S_3} - F_{S_2} \\ m_{c_2}\dot{v}_{c_2} &= F_{c_2} + F_{S_4} - F_{S_3} \\ m_2\dot{v}_2 &= F_2 - F_{S_4} \end{aligned} \tag{3}$$

The constraint equations are obtained by equating the joint accelerations,

$$\begin{aligned}
&v_{S_1} = v_1 + \omega_1^{\times} r_1 = v_{c_1} + \omega_{c_1}^{\times} r_{c_{11}} \\
&\dot{v}_1 + C_1^N \dot{\omega}_1^{\times} r_1 + C_1^N \omega_1^{\times\times} r_1 = \dot{v}_{c_1} + C_{c_1}^N \dot{\omega}_{c_1}^{\times} r_{c_{11}} + C_{c_1}^N \omega_{c_1}^{\times\times} r_{c_{11}} \\
&\Rightarrow \dot{v}_{c_1} - \dot{v}_1 = C_1^N \dot{\omega}_1^{\times} r_1 + C_1^N \omega_1^{\times\times} r_1 - C_{c_1}^N \dot{\omega}_{c_1}^{\times} r_{c_{11}} - C_{c_1}^N \omega_{c_1}^{\times\times} r_{c_{11}} \\
&v_{S_2} = v_{c_1} + \omega_{c_1}^{\times} r_{c_{12}} = v_L + \omega_L^{\times} r_{L_1} \\
&\dot{v}_{c_1} + C_{c_1}^N \dot{\omega}_{c_1}^{\times} r_{c_{12}} + C_{c_1}^N \omega_{c_1}^{\times\times} r_{c_{12}} = \dot{v}_L + C_L^N \dot{\omega}_L^{\times} r_{L_1} + C_L^N \omega_L^{\times\times} r_{L_1} \\
&\Rightarrow \dot{v}_L - \dot{v}_{c_1} = C_{c_1}^N \dot{\omega}_{c_1}^{\times} r_{c_{12}} + C_{c_1}^N \omega_{c_1}^{\times\times} r_{c_{12}} - C_L^N \dot{\omega}_L^{\times} r_{L_1} - C_L^N \omega_L^{\times\times} r_{L_1} \\
&v_{S_3} = v_L + \omega_L^{\times} r_{L_2} = v_{c_2} + \omega_{c_2}^{\times} r_{c_{21}} \\
&\dot{v}_L + C_L^N \dot{\omega}_L^{\times} r_{L_2} + C_L^N \omega_L^{\times\times} r_{L_2} = \dot{v}_{c_2} + C_{c_2}^N \dot{\omega}_{c_2}^{\times} r_{c_{21}} + C_{c_2}^N \omega_{c_2}^{\times\times} r_{c_{21}} \\
&\Rightarrow \dot{v}_{c_2} - \dot{v}_L = C_L^N \dot{\omega}_L^{\times} r_{L_2} + C_L^N \omega_L^{\times\times} r_{L_2} - C_{c_2}^N \dot{\omega}_{c_2}^{\times} r_{c_{21}} - C_{c_2}^N \omega_{c_2}^{\times\times} r_{c_{21}} \\
&v_{S_4} = v_{c_2} + \omega_{c_2}^{\times} r_{c_{22}} = v_2 + \omega_2^{\times} r_2 \\
&\dot{v}_{c_2} + C_{c_2}^N \dot{\omega}_{c_2}^{\times} r_{c_{22}} + C_{c_2}^N \omega_{c_2}^{\times\times} r_{c_{22}} = \dot{v}_2 + C_2^N \dot{\omega}_2^{\times} r_2 + C_2^N \omega_2^{\times\times} r_2 \\
&\Rightarrow \dot{v}_2 - \dot{v}_{c_2} = C_{c_2}^N \dot{\omega}_{c_2}^{\times} r_{c_{22}} + C_{c_2}^N \omega_{c_2}^{\times\times} r_{c_{22}} - C_2^N \dot{\omega}_2^{\times} r_2 - C_2^N \omega_2^{\times\times} r_2
\end{aligned} \tag{4}$$

In vector-matrix form, these equations may be written as:

$$\begin{bmatrix} A & 0 & R \\ 0 & M & U \\ R^T & U^T & 0 \end{bmatrix} \begin{Bmatrix} \dot{x} \\ \dot{y} \\ f \end{Bmatrix} = \begin{Bmatrix} \tau \\ \upsilon \\ \vartheta \end{Bmatrix} \tag{5}$$

where

$$A = \begin{bmatrix} J_1 & 0 & 0 & 0 & 0 & 0 \\ 0 & J_{c_1} & 0 & 0 & 0 & 0 \\ 0 & 0 & J_L & 0 & 0 & 0 \\ 0 & 0 & 0 & J_{c_2} & 0 & 0 \\ 0 & 0 & 0 & 0 & J_2 & 0 \\ 0 & 0 & 0 & 0 & 0 & m_1 I \end{bmatrix}, \quad R = \begin{bmatrix} -r_1^{\times} C_N^1 & 0 & 0 & 0 \\ r_{c_{11}}^{\times} C_N^{c_1} & -r_{c_{12}}^{\times} C_N^{c_1} & 0 & 0 \\ 0 & r_{L_1}^{\times} C_N^L & -r_{L_2}^{\times} C_N^L & 0 \\ 0 & 0 & r_{c_{21}}^{\times} C_N^{c_2} & r_{c_{22}}^{\times} C_N^{c_2} \\ 0 & 0 & 0 & r_2^{\times} C_N^2 \\ -I & 0 & 0 & 0 \end{bmatrix} \tag{6}$$

$$M = \begin{bmatrix} m_{c_1} I & 0 & 0 & 0 \\ 0 & m_L I & 0 & 0 \\ 0 & 0 & m_{c_2} I & 0 \\ 0 & 0 & 0 & m_2 I \end{bmatrix}, \quad U = \begin{bmatrix} I & -I & 0 & 0 \\ 0 & I & -I & 0 \\ 0 & 0 & I & -I \\ 0 & 0 & 0 & I \end{bmatrix} \tag{7}$$

$$\tau = \begin{Bmatrix} T_1 - \omega_1^{\times} J_1 \omega_1 + T_{S_1} \\ T_{c_1} - \omega_{c_1}^{\times} J_{c_1} \omega_{c_1} - C_1^{c_1} T_{S_1} + T_{s_2} \\ T_L - \omega_L^{\times} J_L \omega_L - C_{c_1}^{L} T_{s_2} + T_{s_3} \\ T_{c_2} - \omega_{c_2}^{\times} J_{c_2} \omega_{c_2} - C_L^{c_2} T_{S_3} + T_{s_4} \\ T_2 - \omega_2^{\times} J_2 \omega_2 - C_{c_2}^{2} T_{S_4} \\ F_1 \end{Bmatrix}, \quad \upsilon = \begin{Bmatrix} F_{c_1} \\ F_L \\ F_{c_2} \\ F_2 \end{Bmatrix}, \quad \vartheta = \begin{Bmatrix} C_1^N \omega_1^{\times\times} r_1 - C_{c_1}^N \omega_{c_1}^{\times\times} r_{c_{11}} \\ C_{c_1}^N \omega_{c_1}^{\times\times} r_{c_{12}} - C_L^N \omega_L^{\times\times} r_{L_1} \\ C_L^N \omega_L^{\times\times} r_{L_2} - C_{c_2}^N \omega_{c_2}^{\times\times} r_{c_{21}} \\ C_{c_2}^N \omega_{c_2}^{\times\times} r_{c_{22}} - C_2^N \omega_2^{\times\times} r_2 \end{Bmatrix} \tag{8}$$

$$\dot{x} = \begin{Bmatrix} \dot{\omega}_1 \\ \dot{\omega}_{c_1} \\ \dot{\omega}_L \\ \dot{\omega}_{c_2} \\ \dot{\omega}_2 \\ \dot{v}_1 \end{Bmatrix}, \quad \dot{y} = \begin{Bmatrix} \dot{v}_{c_1} \\ \dot{v}_L \\ \dot{v}_{c_2} \\ \dot{v}_2 \end{Bmatrix}, \quad f = \begin{Bmatrix} F_{S_1} \\ F_{s_2} \\ F_{S_3} \\ F_{S_4} \end{Bmatrix} \tag{9}$$

$\dot{x}, \dot{y}$ and f can be decoupled in equation (5) by introducing unknown coefficient matrices α and β and performing row operations:

$$\left(A + \beta R^T\right)\dot{x} + \left(\alpha M + \beta U^T\right)\dot{y} + \left(R + \alpha U\right) f = \tau + \alpha\upsilon + \beta\vartheta \tag{10}$$

Choose, $\alpha = -RU^{-1}, \quad \beta = RU^{-1}MU^{-T}$, then,

$$\left(A + \beta R^T\right)\dot{x} = \tau + \alpha\upsilon + \beta\vartheta \tag{11}$$

Once the above equation (11) is solved for $\dot{x}$ then $\dot{y}$ and f can be easily computed from Equation (5).

B. Three Quadrotors with a Suspended Load

The same assumptions and approach used for the two quadrotor case is also used in modelling the three quadrotor with a suspended load case. Newton-Euler equations are written for 7 bodies, made of three quadrotors, a suspended load and three rigid cables (Figure 2). Constraint equations are written for the 6 spherical joints connecting the rigid cables to each of the quadrotors to the load.

III. Quadrotor Modeling and LQT Controller Design

A. Quadrotor Model

The general equations of motion of the first quadrotor are written using the newton-euler equations[8].

$$\begin{aligned} \sum F_{ext} &= m_{quad1}\dot{v}_{quad1} + \omega_{quad1}{}^{x} m_{quad1} v_{quad1} \\ \sum M_{ext} &= J_{quad1}\dot{\omega}_{quad1} + \omega_{quad1}{}^{x} J_{quad1}\omega_{quad1} \end{aligned} \tag{12}$$

$$\sum F_{ext} = F_{gravity} + F_{prop} + F_{aero} = C_N^1 m \begin{bmatrix} 0 \\ 0 \\ g \end{bmatrix} - \begin{bmatrix} 0 \\ 0 \\ U_1 \end{bmatrix} - K_t v_{quad1} \tag{13}$$

$$\sum M_{ext} = \begin{bmatrix} U_2 d \\ U_3 d \\ U_4 \end{bmatrix} \tag{14}$$

Using Equations (12)-(14), and carrying out necessary simplications[8], we obtain the following translation and rotation equations for the quadrotor. The translational velocities in Eq. (15) and (17) are written in the inertial frame.[8]

$$\begin{aligned}
\begin{bmatrix} \dot{v}_x \\ \dot{v}_y \\ \dot{v}_z \end{bmatrix} &= \begin{bmatrix} 0 \\ 0 \\ g \end{bmatrix} - C_1^N \begin{bmatrix} 0 \\ 0 \\ U_1 / m_1 \end{bmatrix} - (\mathrm{K_t} / \mathrm{m_1}) \begin{bmatrix} v_x \\ v_y \\ v_z \end{bmatrix} \\
\begin{bmatrix} \dot{p} \\ \dot{q} \\ \dot{r} \end{bmatrix} &= \begin{bmatrix} (I_x - I_z)\,\mathrm{qr/ I_x} \\ (\mathrm{I_z - I_x})\,\mathrm{pr/ I_y} \\ (\mathrm{I_x - I_y})\,\mathrm{pq/ I_z} \end{bmatrix} + \begin{bmatrix} U_2 d / I_x \\ U_3 d / I_y \\ U_4 / I_z \end{bmatrix} \\
\begin{bmatrix} \dot{\phi} \\ \dot{\theta} \\ \dot{\psi} \end{bmatrix} &= \begin{bmatrix} 1 & \sin(\phi)\tan(\theta) & \cos(\phi)\tan(\theta) \\ 0 & \cos(\phi) & -\sin(\phi) \\ 0 & \sin(\phi)/\cos(\theta) & \cos(\phi)/\cos(\theta) \end{bmatrix} \begin{bmatrix} p \\ q \\ r \end{bmatrix}
\end{aligned} \tag{15}$$

$$\begin{aligned} U_1 &= f_1 + f_2 + f_3 + f_4 \\ U_2 &= f_4 - f_2 \\ U_3 &= f_1 - f_3 \\ U_4 &= t_1 + t_3 - t_2 - t_4 \end{aligned} \qquad K_t = \begin{bmatrix} k_x & 0 & 0 \\ 0 & k_y & 0 \\ 0 & 0 & k_z \end{bmatrix} \tag{16}$$

These equations are linearized to be used in linear tracking controller as follows:

$$A_{long}=\begin{bmatrix}-k_x/m_1 & 0 & 0 & -g\\ 0 & -k_z/m_1 & 0 & 0\\ 0 & 0 & 0 & 0\\ 0 & 0 & 1 & 0\end{bmatrix},\ B_{long}=\begin{bmatrix}0 & 0\\ -1/m_1 & 0\\ 0 & d/I_y\\ 0 & 0\end{bmatrix},\ x_{long}=\begin{bmatrix}v_x\\ v_z\\ q\\ \theta\end{bmatrix},\ \mathrm{u}_{\mathrm{long}}=\begin{bmatrix}U_1\\ U_3\end{bmatrix}$$

$$A_{late}=\begin{bmatrix}-k_y/m_1 & 0 & 0 & g & 0\\ 0 & 0 & 0 & 0 & 0\\ 0 & 0 & 0 & 0 & 0\\ 0 & 1 & 0 & 0 & 0\\ 0 & 0 & 1 & 0 & 0\end{bmatrix},\ B_{late}=\begin{bmatrix}0 & 0\\ d/I_x & 0\\ 0 & 1/I_z\\ 0 & 0\\ 0 & 0\end{bmatrix},\ x_{late}=\begin{bmatrix}v_y\\ p\\ r\\ \phi\\ \psi\end{bmatrix},\ u_{late}=\begin{bmatrix}U_2\\ U_4\end{bmatrix} \tag{17}$$

Same approach is used in modelling the second quadrotor as well. The simulations where the controllers are tested are based on the nonlinear equations. Those linearized equations presented in this section are used to design the LQT controller to be tested against the nonlinear model in section II.

B. LQT Controller Design

Given the following linear completely controllable and observable system[9],

$$\dot{\mathbf{x}}(\mathrm{t})=\mathbf{A}(t)\,\mathrm{x}(t)+\mathbf{B}(t)\mathbf{u}(t) \tag{18}$$

$$\mathbf{y}(t)=\mathbf{C}(t)x(t) \tag{19}$$

Find the controller that minimizes the following performance index:

$$\lim_{t_f\to\infty} J=\lim_{t_f\to\infty}\frac{1}{2}\int_{t_0}^{t_f}[\mathbf{e}^t(t)\mathbf{Q}(t)\mathbf{e}(t)+\mathbf{u}^t(t)\mathbf{R}(t)\mathbf{u}(t)]dt \tag{20}$$

Where, the desired output $\mathbf{z}(t)$, the error, $\mathbf{e}(\mathrm{t})=\mathbf{z}(t)-\mathbf{y}(t)$, yield the following algebraic Ricatti equation, and the auxiliary eqution to be solved.

$$-\mathbf{PA}-\mathbf{A}^t\mathbf{P}+\mathbf{PBR}^{-1}\mathbf{B}^t\mathbf{P}-\mathbf{C}^t\mathbf{QC}=\mathbf{0} \tag{21}$$

$$\mathbf{g}(t)=[\mathbf{PE}-\mathbf{A}^t]^{-1}\mathbf{Wz}(t) \tag{22}$$

where,

$$\mathbf{E}=\mathbf{BR}^{-1}\mathbf{B}^t \tag{23}$$

$$\mathbf{W}=\mathbf{C}^t\mathbf{Q} \tag{24}$$

Then the optimal control law becomes:

$$\mathbf{u}(t)=-\mathbf{R}^{-1}\mathbf{B}^t[\mathbf{Px}(t)-\mathbf{g}(t)] \tag{25}$$

or,

$$\mathbf{u}(t)=\mathbf{Kx}(t)+\mathbf{K}_Z\mathbf{z}(t) \tag{26}$$

where

$$\begin{aligned}\mathbf{K}&=-\mathbf{R}^{-1}\mathbf{B}^t\\ \mathbf{K}_Z&=\mathbf{R}^{-1}\mathbf{B}[\mathbf{PE}-\mathbf{A}^t]^{-1}\mathbf{W}\end{aligned} \tag{27}$$

$\mathbf{K}$ and $\mathbf{K}_Z$ are the controller gains for a linear quadratic optimal tracking controller. The linear model in equation (17) is used in designing our LQT controller.

IV. Lyapunov Function based Formation Guidance Controller

The Lyapunov stability theorem states that: Let $x=0$ be an equilibrium point of a nonlinear system $\dot{x}=f(x)$. Let $V: D \rightarrow R$ be a continuously differentiable function in the neighborhood D of $x=0$, such that $V(0)=0$ and $V(x)>0$ in $D-\{0\}$. If $\dot{V}(x)\leq 0$, then $x=0$ is stable. Moreover, if $\dot{V}(x)<0$ in $D-\{0\}$, then $x=0$ is asymptotically stable.[10]

The Lyapunov stability theorem approach may be used to design stabilizing controllers for nonlinear systems.[10] It may also be used to develop a guidance scheme. Here, we employ the approach to guide the follower quadrotor. It is desired that the two quadrotors match their headings and fly at a desired relative distance from each other. Of the two quadrotors, one is designated as leader flown on the desired trajectory using an LQT controller. The other quadrotor is designated as follower, and the Lyapunov based formation controller is implemented to enable the follower track the desired reference relative position to the leader quadrotor. Consider the following Lyapunov function:

$$V=\frac{1}{2}\{\Delta x \quad \Delta y \quad \Delta z \quad \Delta\psi\} Q \begin{Bmatrix} \Delta x \\ \Delta y \\ \Delta z \\ \Delta\psi \end{Bmatrix} \tag{28}$$

Where,

$$\begin{aligned} \Delta x &= x_L + a - x_F \\ \Delta y &= y_L + b - y_F \\ \Delta z &= z_L + c - z_F \\ \Delta\psi &= \psi_L - \psi_F \end{aligned} \tag{29}$$

(x_L, y_L, z_L) and (x_F, y_F, z_F) are the positions of the leader and the follower quadrotors with respect to the inertial frame. (a,b,c) is the desired relative position of the follower with respect to the leader quadrotor. ψ_L, ψ_F are the leader and follower headings. The derivative of the Lyapunov function gives,

$$\dot{V}=(\Delta x \ \Delta y \ \Delta z \ \Delta\psi) Q \begin{Bmatrix} \Delta\dot{x} \\ \Delta\dot{y} \\ \Delta\dot{z} \\ \Delta\dot{\psi} \end{Bmatrix} = -(\Delta x \ \Delta y \ \Delta z \ \Delta\psi)\mathrm{R} \begin{Bmatrix} \Delta x \\ \Delta y \\ \Delta z \\ \Delta\psi \end{Bmatrix} \tag{30}$$

$\Rightarrow$

$$\begin{Bmatrix} \Delta\dot{x} \\ \Delta\dot{y} \\ \Delta\dot{z} \\ \Delta\dot{\psi} \end{Bmatrix} = -Q^{-1}R \begin{Bmatrix} \Delta x \\ \Delta y \\ \Delta z \\ \Delta\psi \end{Bmatrix} \tag{31}$$

From equation (31), the reference signal going from the Lyapunov based formation guidance controller to the follower quadrotor is then:

$$\begin{Bmatrix} V_{x_F} \\ V_{y_F} \\ V_{z_F} \\ \dot{\psi}_F \end{Bmatrix}_{ref} = \begin{Bmatrix} V_{x_L} \\ V_{y_L} \\ V_{z_L} \\ \dot{\psi}_L \end{Bmatrix} + Q^{-1}R \begin{Bmatrix} \Delta x \\ \Delta y \\ \Delta z \\ \Delta \psi \end{Bmatrix} + \begin{Bmatrix} \dot{a} \\ \dot{b} \\ \dot{c} \\ 0 \end{Bmatrix} \quad (32)$$

Although for quadrotors, heading control is not necessary, here it is implemented to prevent cable entanglement.

V. Results and Discussion

A. Two Quadrotors With a Suspended Load

A nonlinear simulation code based on the equations presented above is developed. The properties of the identical quadrotors are presented in Table 1. The nonlinear quadrotor equations of motion are linearized and a LQT controller is designed to track velocity commands in the 3-directions as well as a heading command. This controller is then tested against the nonlinear two quadrotor-slung load model coupled with the Lyapunov based formation controller is used to guide the follower quadrotor. It is desired that the follower flies at the same altitude as the leader but one meter to the left of the follower $(x_F - x_L, y_F - y_L, z_F - z_L) = (0,1,0)$. The controller gains used in the simulation are listed in Table 2.

As shown in Figure 3, a reference velocity given to the leader quadrotor and the response of the leader quadrotor are presented. From the figure, it may be observed that the quadrotor follows the reference commands quite closely. The disturbance from the slung load is also observable in the plots. Figure 4 gives the position of the two quadrotors and the load in three dimensions. The errors associated with the leader trajectory and the follower quadrotor trajectory are presented in Figure 5. It may be observed from this figure that the follower tracks the leader quite closely. Maximum position errors in the the x, y, and z directions are less then 0.5m, 0.05m and 0.02 m respectively. The load is also following the quadrotors with swinging, rocking and yawing motion (Figure 6). This rocking and swinging motion is more pronounced at the beginning when there is a sudden jerk applied by the quadrotors. The control commands, namely the propeller speeds of the leader and follower quadrotors are presented in Figure 7, and 8. From the figures, it may be observed that there is no saturation in the speeds and the speeds are realizable by the electric motors of the quadrotors. Finally the leader quadrotor velocities in three directions are given in Figure 9. From this figure it may be observed that the leader quadrotor tracks the velocity commands quite closely.

B. Three Quadrotors With a Suspended Load

To test the performance of our three-quadrotor slung load system, the same trajectory as before is commanded to the leader in the formation. It is desired that the initial formation geometry be maintained in spite of the leader quadrotor maneuver. To achieve this, the following relative distances are sent to the guidance algorithms: $(x_{F1} - x_L, y_{F1} - y_L, z_{F1} - z_L) = (-0.5, -0.5, 0)$, and $(x_{F2} - x_L, y_{F2} - y_L, z_{F2} - z_L) = (-0.5, 0.5, 0)$.

Figure 10 gives the positions of all quadrotors and the load in three dimensions. The error in the tracked formation geometry are presented in Figure 11 and 12 for each of the follower quadrotors. From these figures it may be observed that small along track position error is rapidly recovered and errors in lateral and vertical directions on the other are quite small. The load attitude is presented in Figure 13. Comparing this figure with the previous case, one may conclude that, inspite of the larger initial swing in the three quadrotor case, the load flies much more smoothly than the two quadrotor case. Thus, the load rock and heading angles are almost zero and the load swing angle quickly returns to zero after an initial jump to 80 degrees as a result of the climbing motion of the leader quadrotor. The control commands, namely the propeller speeds of the leader and follower quadrotors are presented in Figure 14-16. From these figures, it may be observed that there is no saturation in the propeller speeds and these speeds should be realizable by the electric motors of the quadrotors.

VI. Conclusion

A nonlinear simulation model for two quadrotors carrying a slung load is developed. The quadrotor flight controls is realized by a linear quadratic type controller. A Lyupunov function based formation controller is developed to track relative distances between the quadrotors. The simulation results show that the quadrotors are not destabilized under the disturbance of the slung load. The quadrotors are also able to fly in the desired formation in spite of the slung load. The load follows the quadrotors with some swinging and rocking in the two quadrotor case. However, the load rock and heading angles are reduced in the three quadrotor case due to addition contraints introduced into the system as a result of the additional cable attached to the load.

Table 1. Properties of the quadrotors, cables and load used.

Quadotor mass, m_1, m_2, m_3	0.65 Kg
Load mass, m_L	0.2 Kg
Cable mass, m_{c1}, m_{c2}, m_{c3}	0.01 Kg
Cable length, L_c	1 m
Load Radius, R_L	0.5 m
Thrust Coefficient, of the propellers k_f	$3.43\times10^{-7}\, N/(\text{rpm})^2$
Distance of the propellers from the center of mass, k_i	0.016 m
Inertia Matrices of Quadrotors, J_1, J_2, J_3	$\begin{bmatrix} 7.5\times10^{-3} & 0 & 0 \\ 0 & 7.5\times10^{-3} & 0 \\ 0 & 0 & 1.3\times10^{-2} \end{bmatrix}$
Inertia Matrix of the Load, J_L	$\begin{bmatrix} 2.0\times10^{-2} & 0 & 0 \\ 0 & 2.0\times10^{-2} & 0 \\ 0 & 0 & 2.0\times10^{-2} \end{bmatrix}$
Innertia Matrix of Cables, J_{c1}, J_{c2}, J_{c3}	$\begin{bmatrix} 8.3\times10^{-4} & 0 & 0 \\ 0 & 8.3\times10^{-4} & 0 \\ 0 & 0 & 1.0\times10^{-7} \end{bmatrix}$
Drag coefficient where the drag force is taken proportional to the quadrotor speed	$0.1 \quad N/(m/\text{s})$

Table 2. Controller gains used.

v_x, v_z Controller	v_y, heading Controller
$K_1 = \begin{bmatrix} 0 & 49.9001 & 0 & 0 \\ 0.9551 & 0 & -0.4320 & -2.8618 \end{bmatrix}$	$K_2 = \begin{bmatrix} -0.9551 & -0.4320 & 0 & -2.8618 & 0 \\ 0 & 0 & -0.1612 & 0 & -1 \end{bmatrix}$
$Kz_1 = \begin{bmatrix} 0 & -49.9999 \\ -1 & 0 \end{bmatrix}$	$Kz_2 = \begin{bmatrix} 1 & 0 \\ 0 & 1 \end{bmatrix}$

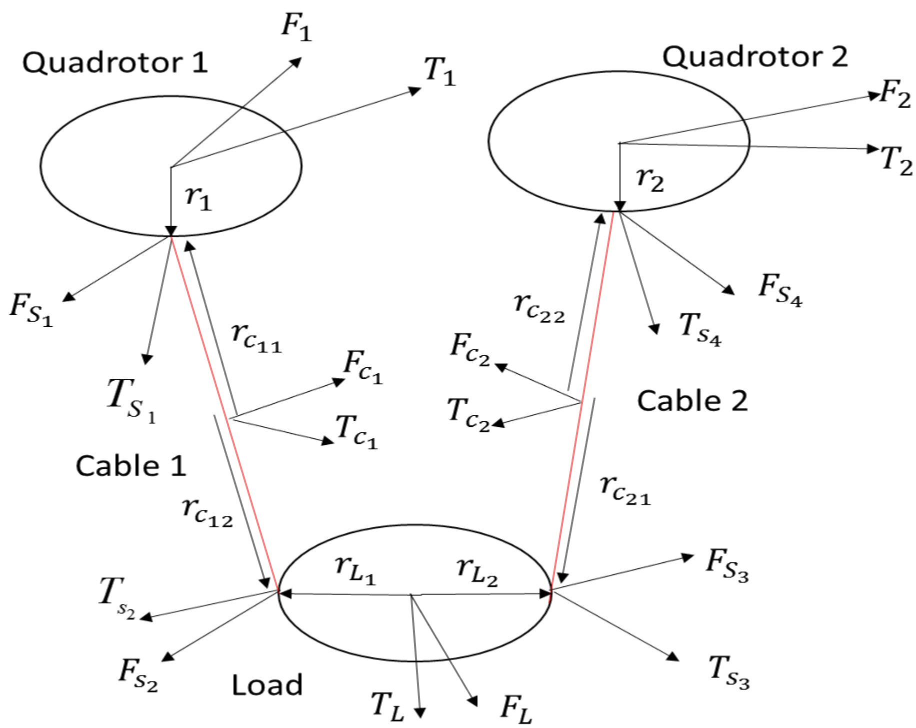

Figure 1. Two quadrotors with a slung load

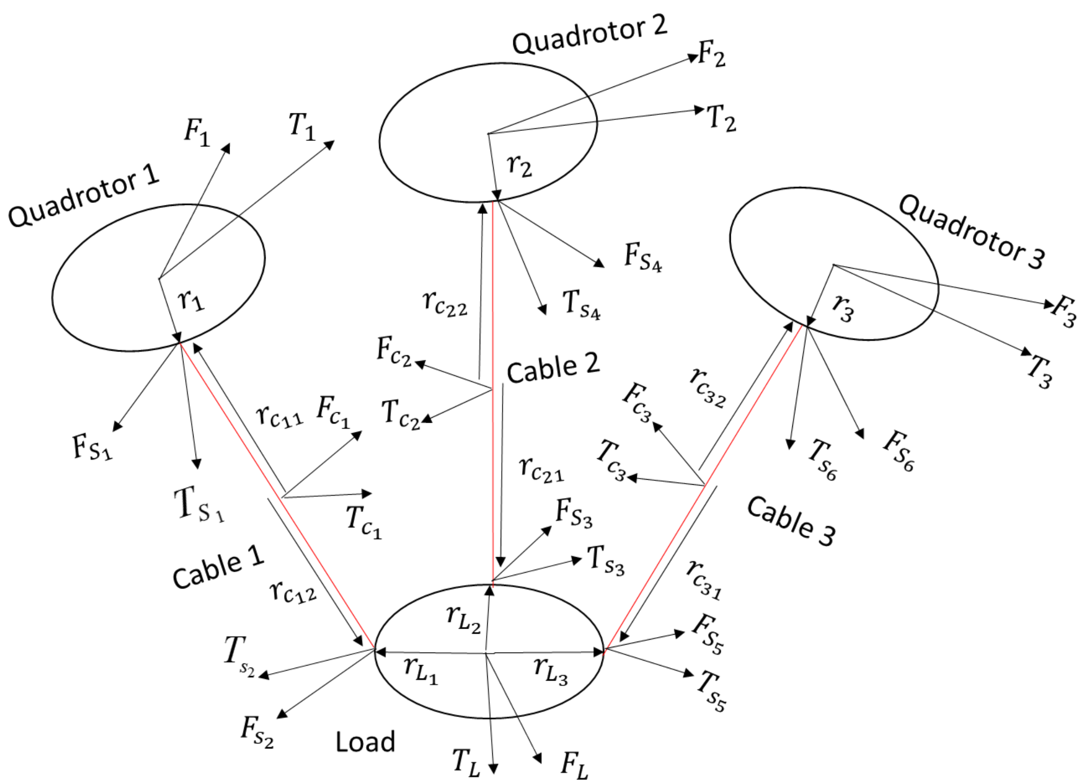

Figure 2. Three quadrotors with a slung load

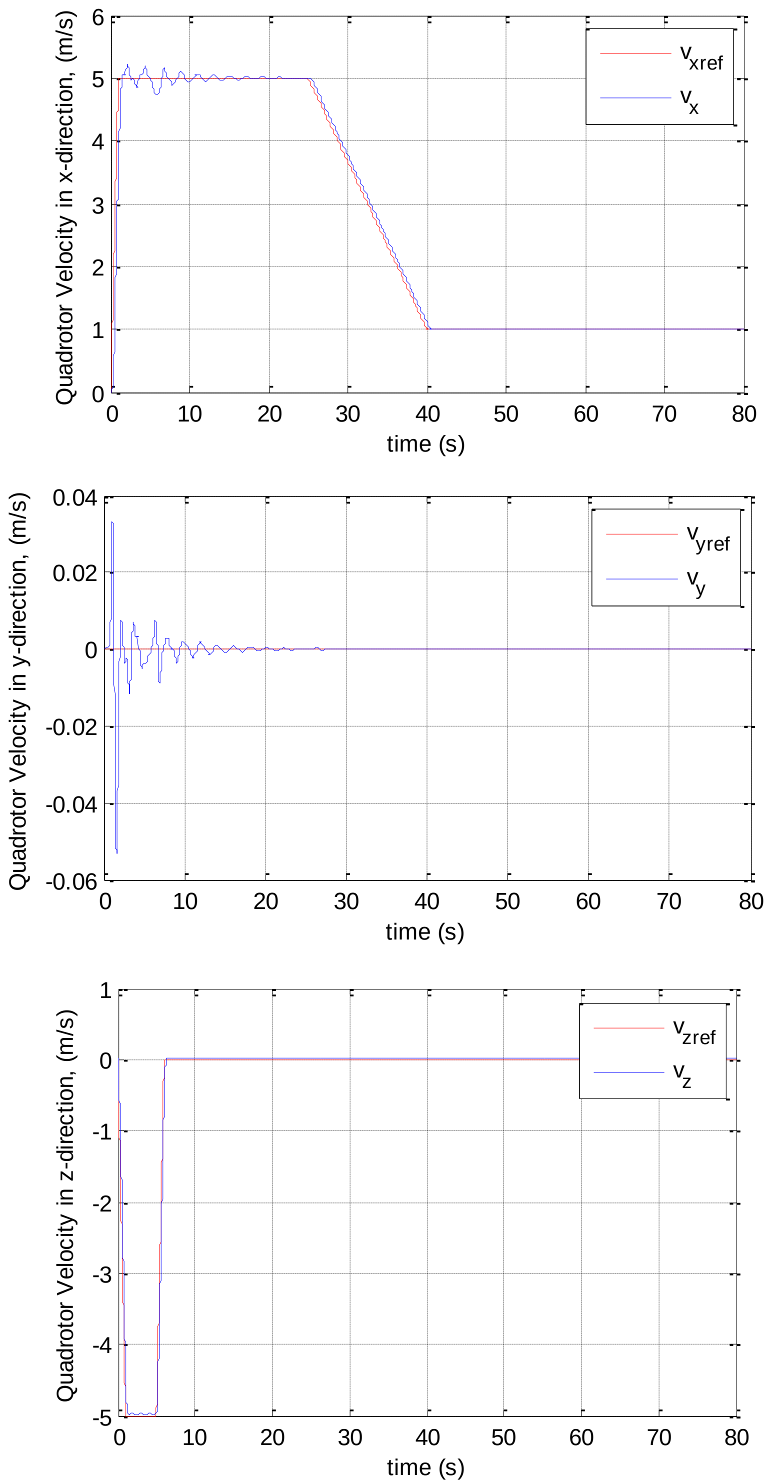

Figure 3. Leader quadrotor velocities in three directions (2 quadrotors case)

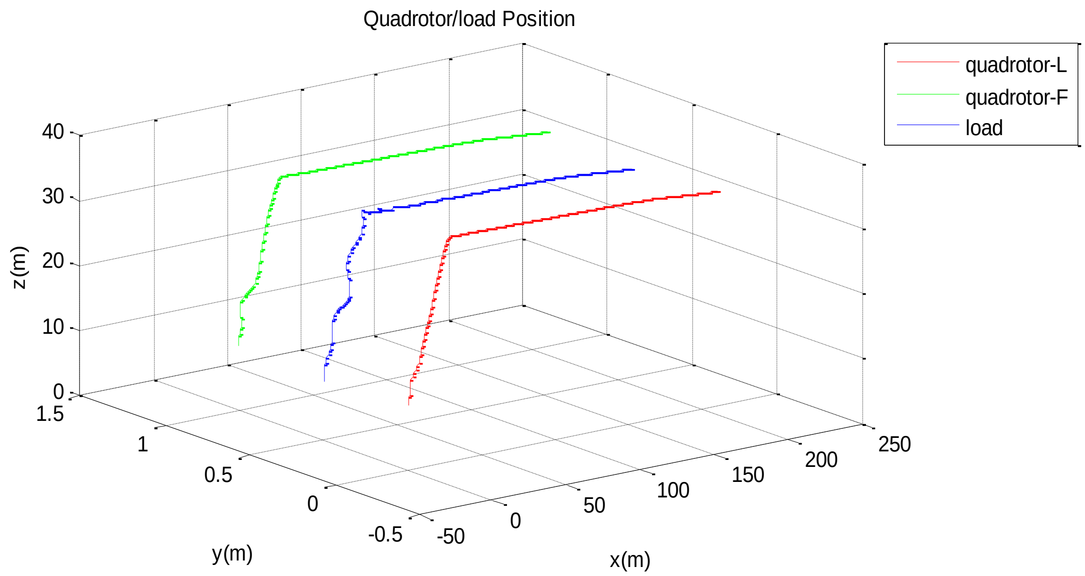

Figure 4. Quadrotor and slung load positions (2 quadrotor case)

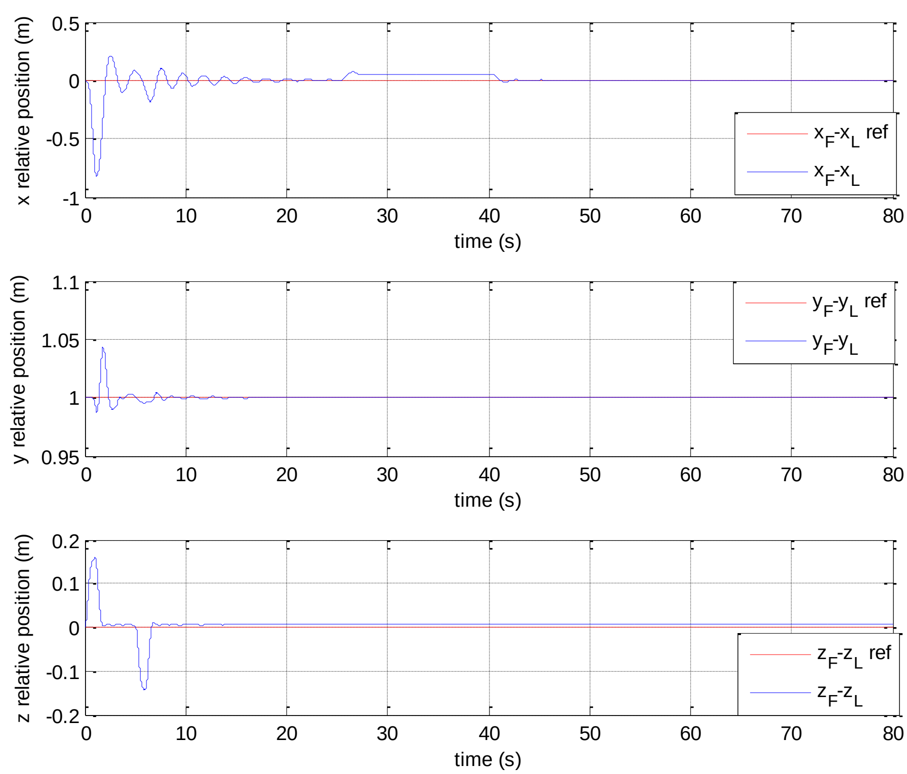

Figure 5. Leader and follower quadrotor relative positions (2 quadrotor case)

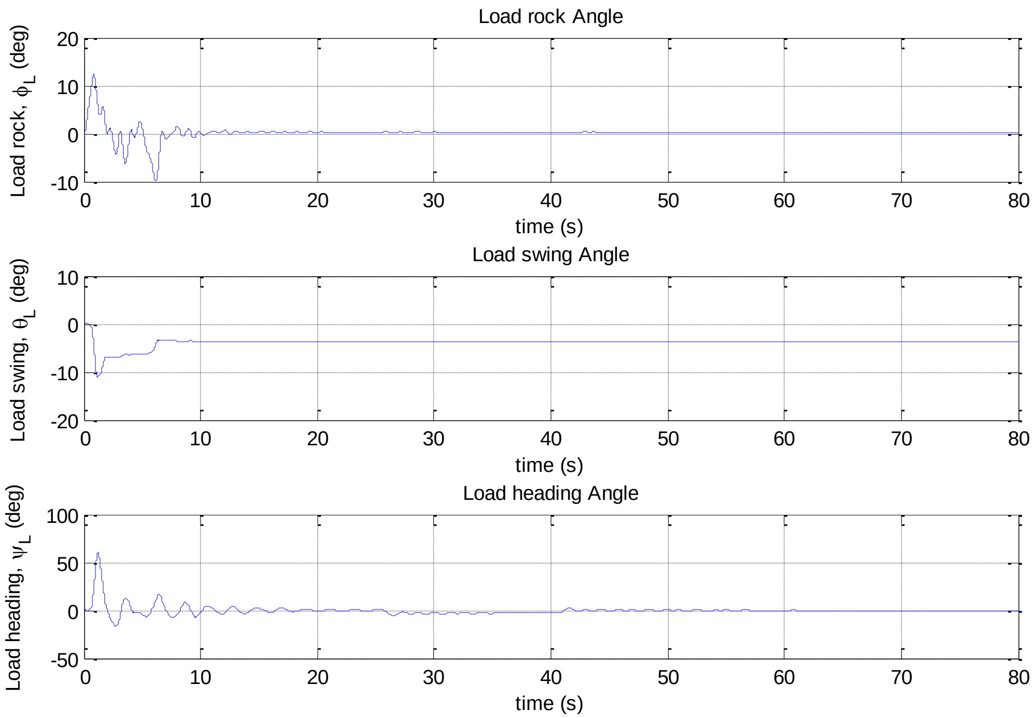

Figure 6. Swing, rock and heading angles of the load (2 quadrotor case)

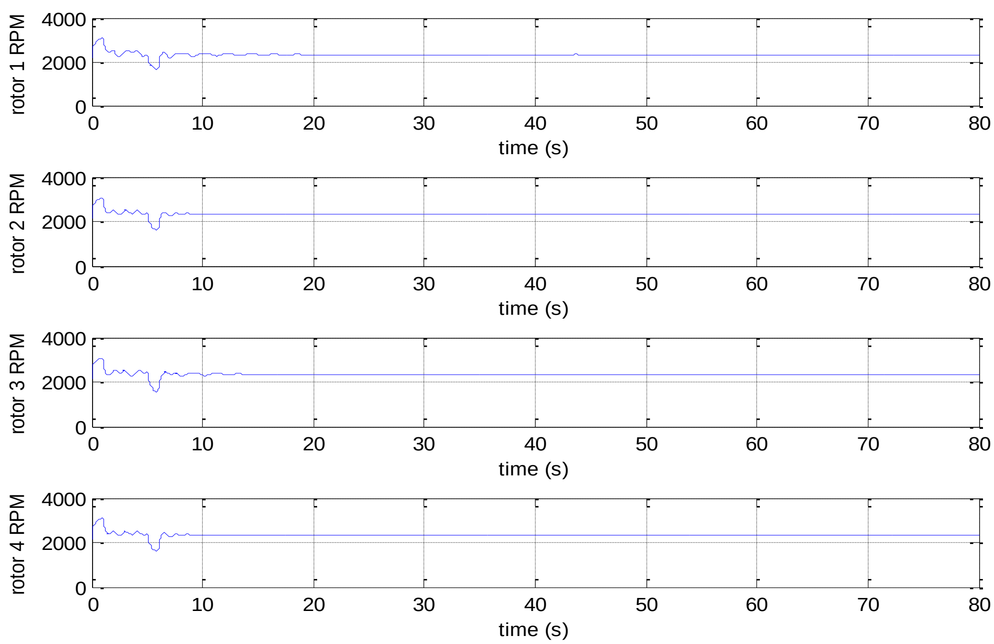

Figure 7. Propeller speeds of Leader Quadrotor (2 quadrotor case)

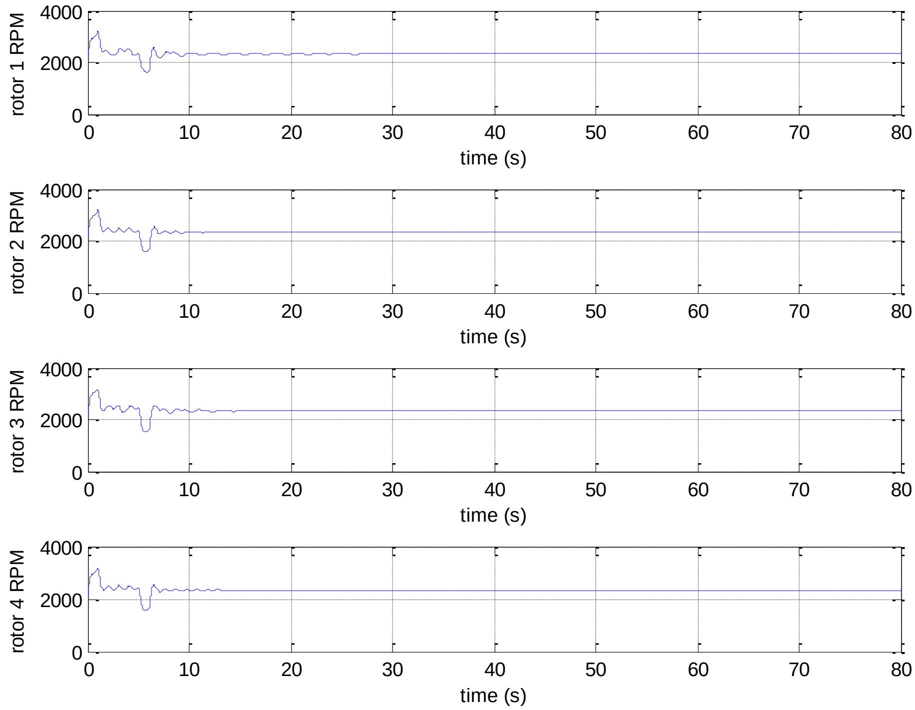

Figure 8. Propeller speeds of Follower Quadrotor (2 quadrotor case)

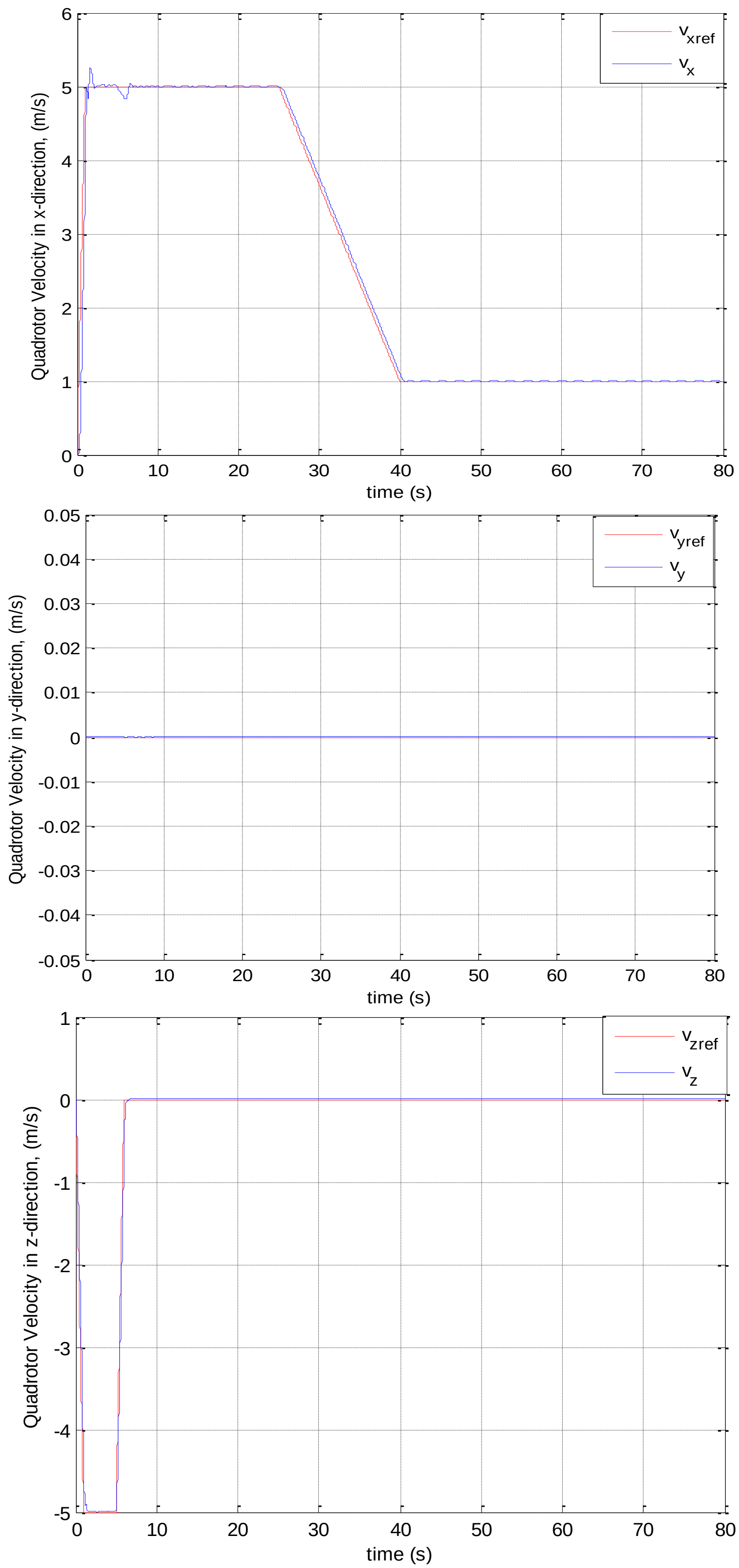

Figure 9. Leader Quadrotor velocities in three directions (2 quadrotor case)

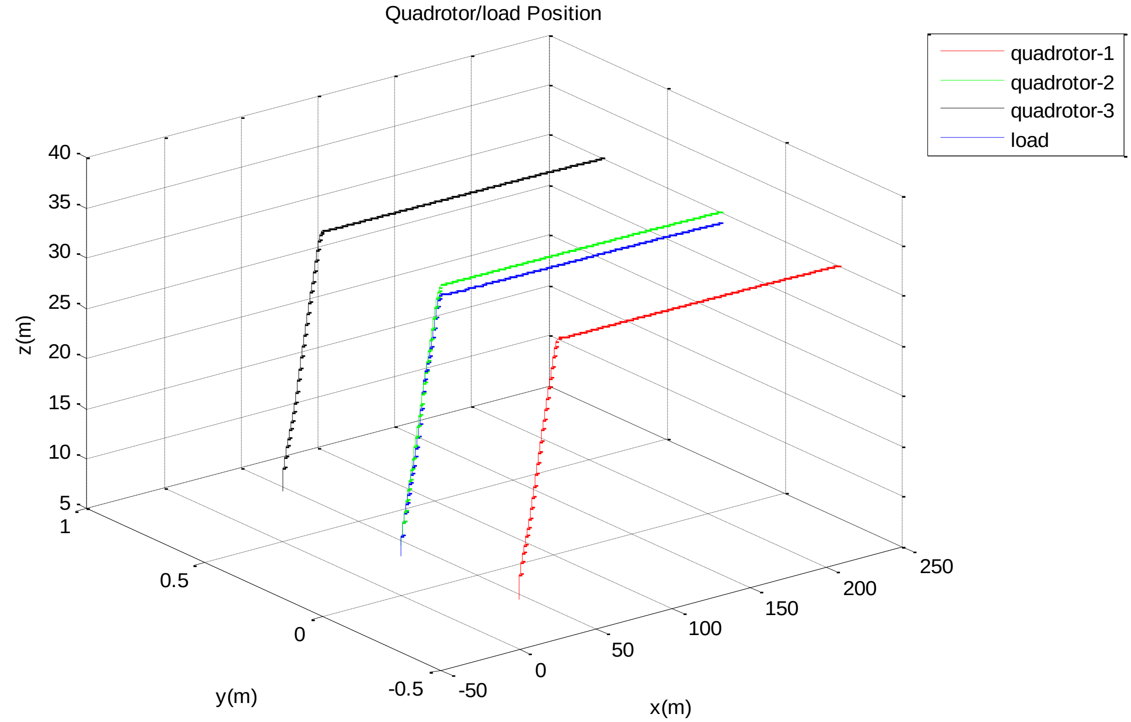

Figure 10. Quadrotor and load positions (3 quadrotor case)

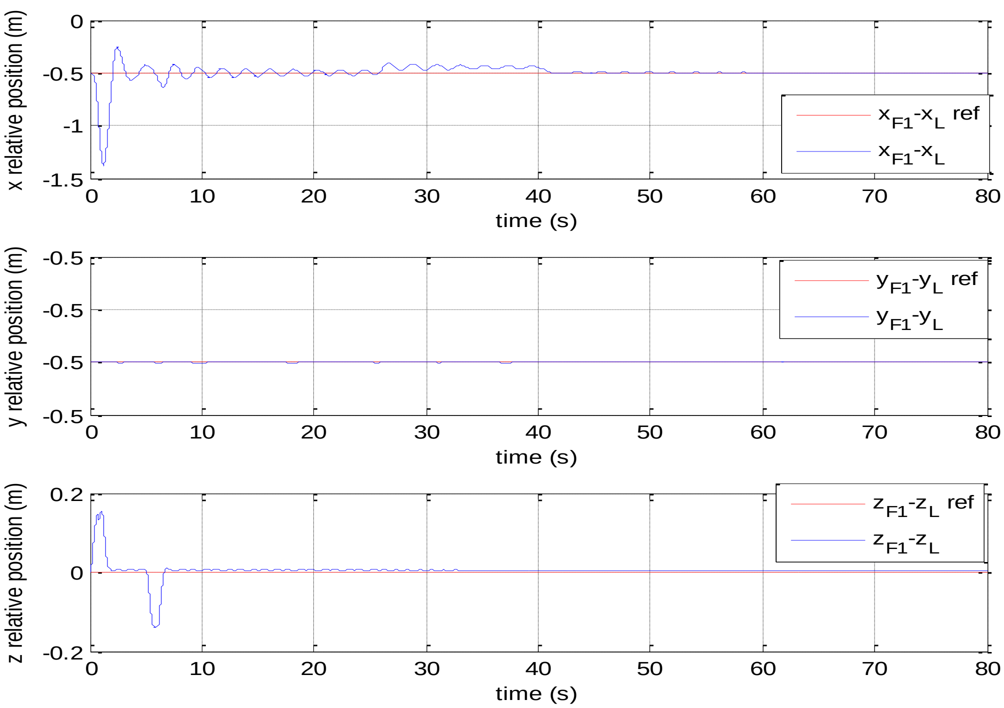

Figure 11. Leader and 1st follower quadrotor relative positions (3 quadrotor case)

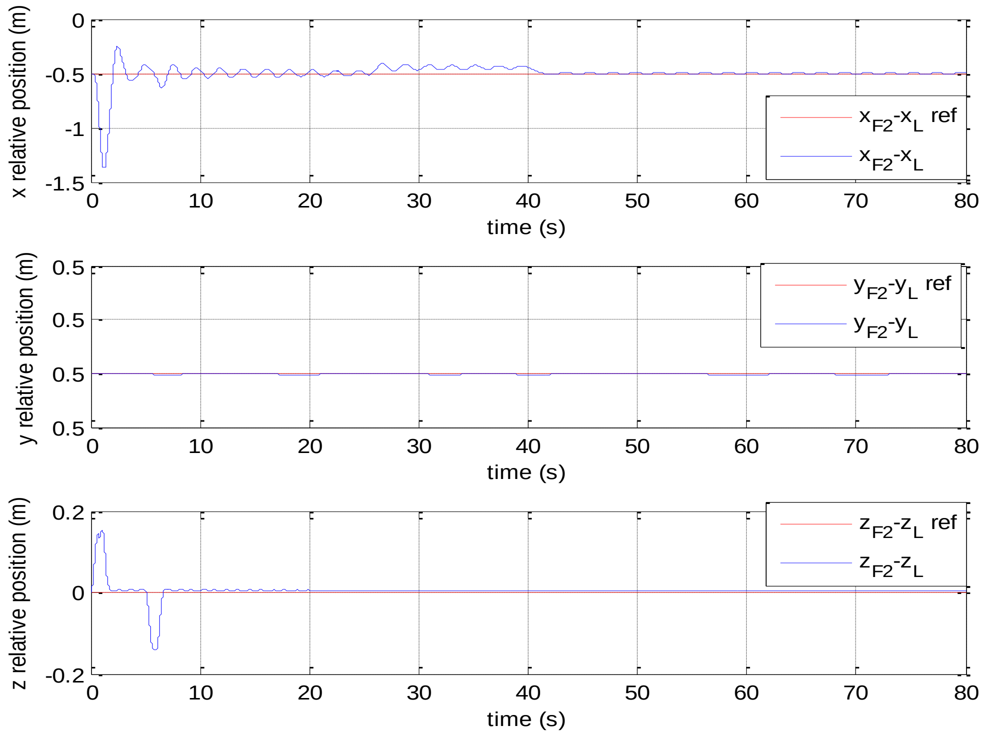

Figure 12. Leader and 2nd follower quadrotor relative positions (3 quadrotor case)

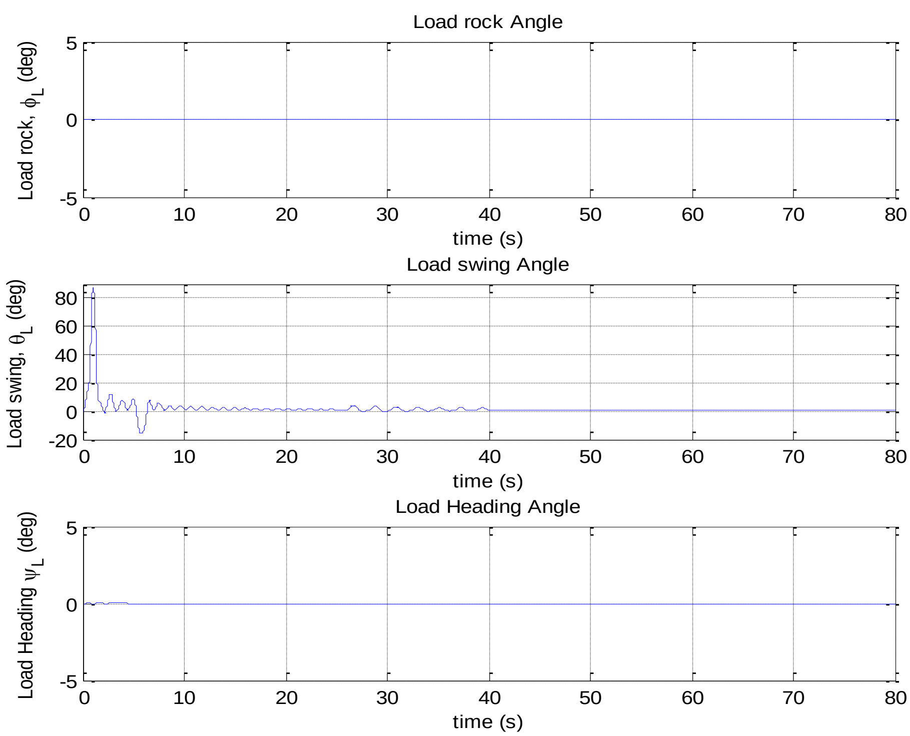

Figure 13. Swing, rock and heading angles of the load (3 quadrotor case)

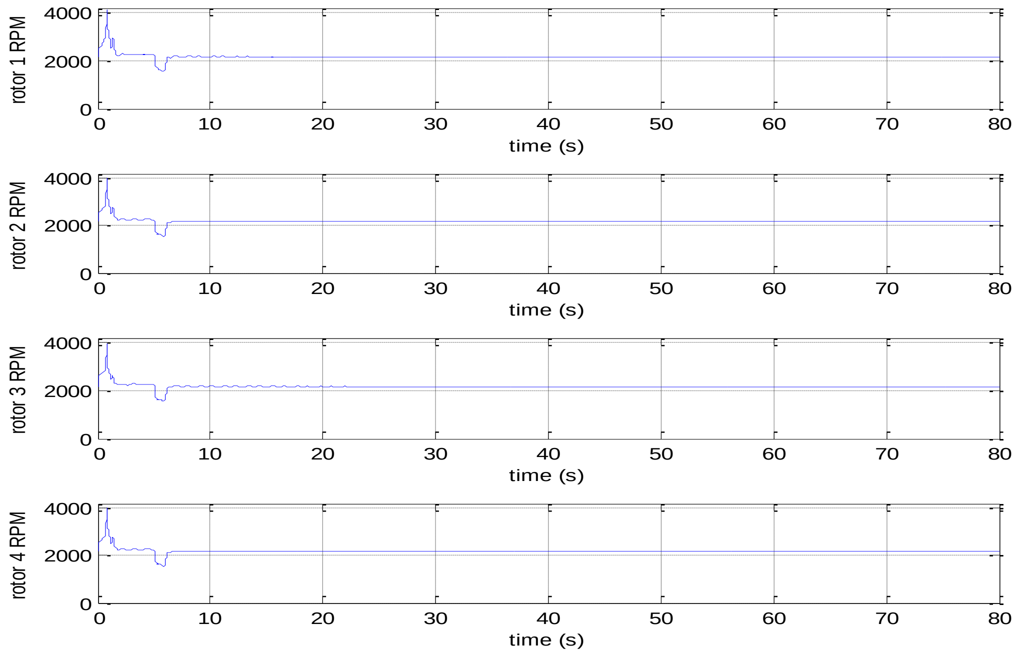

Figure 14. Propeller speeds of the leader quadrotor (3 quadrotor case)

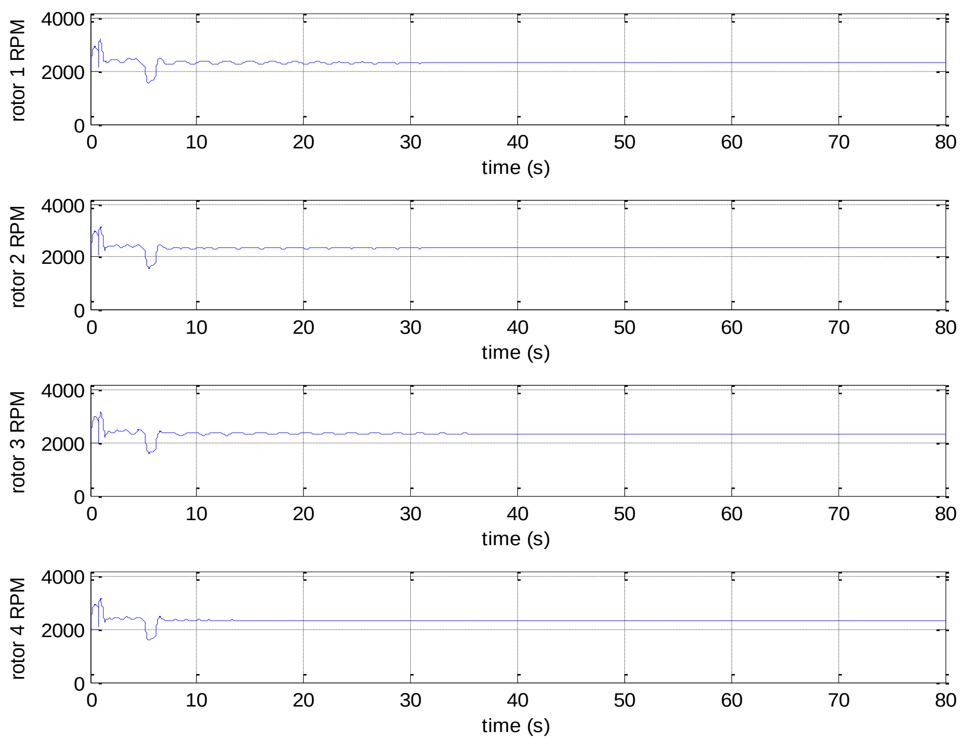

Figure 15. Propeller speeds of the 1st follower quadrotor (3 quadrotor case)

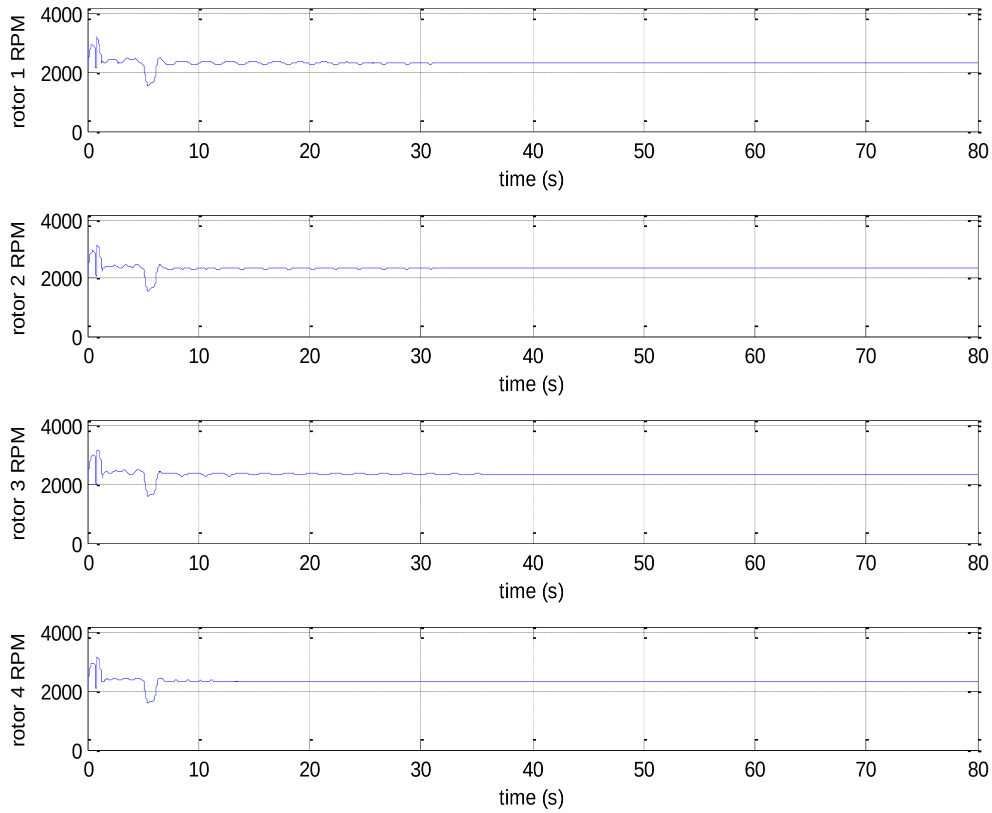

Figure 16. Propeller speeds of 2nd follower quadrotor (3 quadrotor case)

References

[1] Ivana, P., Rafael, F. , Patricio, C. "Trajectory Generation for Swing-Free Maneuvers of a Quadrotor with Suspended Payload: A Dynamic Programming Approach", *IEEE International Conference on Robotics and Automation. River Center*, Saint Paul, Minnesota, USA. May 2012.

[2] Bouabdallah, S., Noth, A. and Siegwart, R., "PID vs LQ control techniques applied to an indoor micro quadrotor." *Intelligent Robots and Systems, 2004.(IROS 2004) Proceedings of 2004 IEEE/RSJ International Conference on*, Vol. 3. 2004.

[3] Dydek, Z. T., Annaswamy, A.M., Lavretsky, E. "Adaptive control of quadrotor UAVs: A design trade study with flight evaluations." *Control Systems Technology*, pp. 1400-1406, 2013.

[4] Zhang, Xiaobing, et al., "Fault Tolerant Control for Quadrotor via Backstepping Approach," *48th AIAA Aerospace Sciences Meeting Including the New Horizons Forum and Aerospace Exposition*, Orlando, Florida, USA. 2010.

[5] Ariyibi, S.O., Tekinalp, O., "Nonlinear Guidance of Unmanned Aircraft Formations," *AIAA SciTech 2015*, Orlando, FL, January 5-9, 2015.

[6] Tekinalp, O., Kumbasar, S., "SDRE Based Guidance and Flight Control of Aircraft Formations," *AIAA SciTech 2015*, Orlando, FL, January 5-9, 2015.

[7] Stoneking, E., "Newton-Euler Dynamic Dynamic Equations of Motion for a Multi-body Spacecraft," *AIAA Guidance, Navigation and Control Conference and Exhibit*, South Carolina, August 2007.

[8] Suicmez, E., *Trajectory Tracking of a Quadrotor Unmanned Aerial Vehicle(UAV) via Attitude and Position Control*, MS. Thesis, Middle East Technical University Libraries, July 2014.

[9] Naidu, D.S., *Optimal Control Systems*, CRC Press LLC, 2003.

[10] Khalil, H.K., *Nonlinear Systems*, Prentice Hall, 2002.